Ralston, E., and Ploug, T. (1996). GLUT4 in cultured skeletal myotubes is segregated from the transferrin receptor and stored in vesicles associated with TGN. J. Cell Sci. 109, 2967–2978.

Ryden, M., Dicker, A., Harmelen, V., et al. (2002). Mapping of early signaling events in tumor necrosis factor-alpha–mediated lipolysis in human fat cells. J. Biol. Chem. 277, 1085–1091.

Slot, J.W., Geuze, H.J., Gigengack, S., et al. (1991). Immuno-localization of the insulin regulatable glucose transporter in brown adipose tissue of the rat. J. Cell Biol. 113, 123–135.

Slot, J.W., Garruti, G., Martin, S., et al. (1997). Glucose transporter (GLUT-4) is targeted to secretory granules in rat atrial cardiomyocytes. J. Cell Biol. 137, 1243–1254.

Sottile, V., Thomson, A., and Mcwhir, J. (2003). *In vitro* osteogenic differentiation of human ES cells. Cloning Stem Cells 5, 149–155.

Thomson, J.A., Kalishman, J., Golos, T.G., et al. (1995). Isolation of a primate embryonic stem cell line. Proc. Natal. Acad. Sci. USA 92, 7844–7848.

Yamashita, A., Takada, T., Narita, J., et al. (2005). Osteoblastic differentiation of monkey embryonic stem cells *in vitro*. Cloning Stem Cells 7, 232–237.

Yamashita, A., Takada, T., Yamamoto G., et al. (2006). Stable maintenance of monkey embryonic stem cells in the absence of bFGF. Transplant. Proc. (in press).

Address reprint requests to:
Dr. Tatsuyuki Takada
Shiga University of Medical Science
Research Center for Animal Life science
Tsukinowa-cho, Seta
Ohtsu, 520-2192 Japan

E-mail: ttakada@belle.shiga-med.ac.jp

PEPTIDES 27 (2006) 1886–1893

available at www.sciencedirect.com

SCIENCE DIRECT®

journal homepage: www.elsevier.com/locate/peptides

Short communication

Molecular cloning of BNP from heart and its immunohistochemical localization in the hypothalamus of monkey

Essam Mohamed Abdelalim [a,b], *Tatsuyuki Takada* [b], *Ryuzo Torii* [b], *Ikuo Tooyama* [a,*]

[a] *Molecular Neuroscience Research Center, Shiga University of Medical Science, Setatsukinowa-cho, Otsu, Shiga 520-2192, Japan*
[b] *Research Center For Animal Life Science, Shiga University of Medical Science, Setatsukinowa-cho, Otsu, Shiga 520-2192, Japan*

ARTICLE INFO

Article history:
Received 18 October 2005
Received in revised form
29 December 2005
Accepted 4 January 2006
Published on line 9 February 2006

Keywords:
Natriuretic peptide
Neuroendocrine
Hypothalamus
Monkey

ABSTRACT

Previous physiological studies have suggested central roles of brain natriuretic peptide (BNP). However, little information is available about the localization of BNP in the brain. In this study, we determined cDNA sequence encoding the entire coding region of prepro-BNP of Japanese and cynomologus monkeys, and then examined the immunohistochemical localization of BNP in the monkey hypothalamus. Japanese and cynomologus monkey prepro-BNP consisted of 132 amino acid residues with biologically active C-terminal 32 amino acids. Comparisons of deduced amino acid sequences among different species revealed high homology between monkey and human (91% in prerpro-BNP and 97% in the mature region). Immunohistochemical examination showed that BNP immunoreactive dots were observed in the paraventricular, periventricular, and supraoptic nuclei of the monkey hypothalamus. The present result suggests the central role of BNP in the neuroendocrine system in the hypothalamus.

1. Introduction

Brain natriuretic peptide (BNP), a member of natriuretic peptide family, is a potent natriuretic, diuretic, and vasorelaxant peptide (for reviews [11,16,17,20]). It was originally isolated from the porcine brain [23]. Then, the nucleotide and amino acid sequences of BNP have been identified for several mammalian species, including human, cattle, sheep, dog, mouse, rat, feline, and camel [1,2,8,10,14,15,18,19,22]. Unlike ANP, BNP has species variations in both its structure and tissue distribution [16,20]. Particularly the human BNP sequence differs from other species. Therefore, it is important to clarify the BNP sequence of monkey that is phylogenetically similar to human.

BNP is mainly synthesized, stored, and released in the ventricular myocardium [20]. A previous study using in situ hybridization reported that BNP mRNA was not detected in the brain [12]. However, physiological studies have demonstrated the possible role of BNP in the brain, particularly in the hypothalamus [7,25]. Previous radioimmunoassay studies reported that BNP was detected in the distinct brain regions including the hypothalamus [6,24]. The high density binding sites for BNP was also reported in the subfornical organ, the supraoptic nucleus (SON), and paraventicular hypothalamic nucleus (PVN) [3]. NPR-A mRNA was found in the subfornical organ [13], that is not separated from the blood by blood–brain barrier. These results suggest that BNP expressed in the heart may enter the brain and play an

* *Corresponding author*. Tel.: +81 77 548 2328; fax: +81 77 548 2402.
E-mail address: kinchan@belle.shiga-med.ac.jp (I. Tooyama).
0196-9781/$ – see front matter © 2006 Elsevier Inc. All rights reserved.
doi:10.1016/j.peptides.2006.01.001

important role in the hypothalamus [9]. However, little information is available about the localization of BNP in the hypothalamus with an exception of rat [21]. Our aim in this study was to clone the coding region of BNP of Japanese monkey (*Macaca fuscata*) and cynomologus monkey (*Macaca fasicularis*), and to investigate the immunohistochemical localization of BNP in the hypothalamus of cynomologus monkey.

2. Materials and methods

2.1. Tissue preparations

Samples were obtained from the heart ventricles (right and left) of two Japanese monkeys (13 and 17 years old) and one cynomologus monkey (the age not determined), as well as hypothalamus of one cynomologus monkey immediately after sacrificing the animals that were used for other research purposes by other researchers. The animal use protocols were approved by the Institutional Animal Care and Use Committee (IACUC) of Shiga University of Medical Science. Specimens were stored frozen at −80 °C until use. For immunohistochemistry, samples were obtained from brain of two cynomologous monkeys (the age not determined) and immediately fixed in 4% paraformaldehyde in 0.1 M phosphate buffer pH 7.4 for 2 days at 4 °C, then subjected to sucrose 15% in 0.1 M phosphate buffer pH 7.4 with 0.1% sodium azide, the sucrose was changed every day for 4 days and then stored in sucrose at 4 °C until sectioning. Fixed tissues were subjected to cryostat sectioning at −20 °C.

2.2. BNP cloning

Total RNA was extracted by using Trizol reagent (Invitrogen Corp. Carlsbad, CA, USA), and then was reverse-transcripted into cDNA using superscript III (Invitrogen). Polymerase chain reaction (PCR) amplification of cDNA was carried out using four BNP primers to get complete coding region sequence. The primers were 5′-ATGGATCCCCAGACAGCACCTTCC-3′ (sense), 5′-TTAATGCCGCCTCAGCACTTTGCA-3′ (antisense), 5′-AGCCTCCGCAGTCCCTCCAGAGAC-3′ (sense), and 5′-AGGTGTCTGCAGCCAGGACTTCCT-3′ (antisense). These primers were designed from human BNP sequence that is available in GenBank with accession no. BC025785. The amplification profile consisted of initial step of denaturation at 95 °C for 10 min, 40 cycles of 30 s at 95 °C, 30 s at 56 °C, and 1 min at 72 °C, followed by a final extension at 72 °C for 10 min. The PCR product was directly sequenced by dideoxynucleotide chain termination reaction and primer-walking methods using automated DNA sequencer.

2.3. Reverse transcription polymerase chain reaction (RT-PCR)

Total RNA was extracted from heart and hypothalamus samples by using Trizol reagent (Invitrogen Corp. Carlsbad), and then was reverse-transcripted into cDNA using super-

```
J.m.   1 ATGGATCCCCAGACAGCACCTTCCCGGGTGCTTCTGCTTCTGCTCTTCTTGCACCTGGCTCTCCCGGGAG 70
                                  ||||||||||||||||||||||||||||||#||||||||||||||||||||||||||||||||||||||||
C.m.   1 ATGGATCCCCAGACAGCACCTTCCCGGGTGCTCCTGCTTCTGCTCTTCTTGCACCTGGCTCTCCCGGGAG 70

J.m.   71 GTCGTTCCCACCCACTGGGCAGTTCGGCCTCGGACTTGGAAACGTCTGGGTTACAGGAGCAGCGCAACCA 140
                                  ||||||||||||||||||||||||||||||||||||||||||||||||||||||||||||||||||||||||
C.m.   71 GTCGTTCCCACCCACTGGGCAGTTCGGCCTCGGACTTGGAAACGTCTGGGTTACAGGAGCAGCGCAACCA 140

J.m.   141 TTTGCAGGGCAAACTCTCAGAGCTGCAGGTGGAGCAGATATCCCTGGAGCCCCCCCAGGAGAGCCCCCGT 210
                                  ||||||||||||||||||||||||||||||||||||||||||||||||||||||||||||||||||||||||
C.m.   141 TTTGCAGGGCAAACTCTCAGAGCTGCAGGTGGAGCAGATATCCCTGGAGCCCCCCCAGGAGAGCCCCCGT 210

J.m.   211 CCCACAGGTATCTGGAAGGCCCAGGAGGCAGCCACTGAGGGCATCCGTGGCCACCGCAAAATGGTCCTGT 280
                                  ||||||||||||||||||||||||||||||||||||||||||||||||||||||||||||||||||||||||
C.m.   211 CCCACAGGTATCTGGAAGGCCCAGGAGGCAGCCACTGAGGGCATCCGTGGCCACCGCAAAATGGTCCTGT 280

J.m.   281 ACACCCTGCGGGCACCGCGAAGCCCCAAGATGGTACGAGGGTCTGGCTGCTTTGGGAGGAAGATGGACCG 350
                                  ||||||||||||||||||||||||||||||||||||||||||||||||||||||||||||||||||||||||
C.m.   281 ACACCCTGCGGGCACCGCGAAGCCCCAAGATGGTACGAGGGTCTGGCTGCTTTGGGAGGAAGATGGACCG 350

J.m.   351 GATCAGCTCCTCCAGCGGCCTGGGCTGCAAAGTGCTGAGGCGGCATTAA 399
                                  ||||||||||||||||||||||||||||||||||||||||||||||||||
C.m.   351 GATCAGCTCCTCCAGCGGCCTGGGCTGCAAAGTGCTGAGGCGGCATTAA 399
```

Fig. 1 – Alignment of nucleotides sequence of the coding region of BNP of Japanese monkey with cynomologus monkey. The coding region was 396 bp in both animals. Note the nucleotides mark with (#) indicates the only difference between both sequences. Underlined TAA is the stop codon.

```
Japanese M.      MDPQTAPSRV LLLLLFLHLA LPGGRSHPLG S--SASDLET SGLQEQRNHL QGK-LSELQV EQISLEPPQE  67
Cynomologus M.   .......... .......... .......... .--....... .......... ...-...... ..........  67
Human            .........A .......... FL........ .PG....... .......... ...-...... ..T....L..  69
Sheep            ....K.L..T .........S .L.C...... GPG...E.P- -....LLDR. RDR-V....A ..LRV..L.Q  67
pig              .G.RM.LP.- V........L .L.C...... GAGL..E.P- -.I..LLDR. RDR-V....A .RTD...LRQ  66
Camel            .G....LP.A ..F......S .L.CL..... GPGP..E.P- -.I..LLDR. RDRVI....A ..MD.K.L.Q  68
cat              ...K..LL.A .........S PL........ GPGP..EAS- -AI..LLDG. RDT-V....E A.MA.G.L.Q  67
Mouse            ..LLKVL.QM I.F....Y.S PL..H..... .PSQSPEQF- -KM.KLLELI RE.-------S .EMAQRQLLK  62

Japanese M.      SPRPTGIWKA QEAATEGIRG HRKMVLYTLR APRSPKMVRG SGCFGRKMDR ISSSSGLGCK VLRRH 132
Cynomologus M.   .......... .......... .......... .......... .......... .......... ..... 132
Human            ......V..S R.V....... .......... ........Q. .......... .......... ..... 134
Sheep            GQGLEET.DS PA..PA.FL. PHHSL.QA.. G---...M.D ......RL.. .G.L.....N ....Y 129
pig              DRGL.EA.E. R...PT.VL. P.SSIFQV.. GI....TM.D ......RL.. .G.L.....N ....Y 131
Camel            GQGLAEA.ET PA.FP.RVT. P.NK..EA.. GI.....M.D .S....RL.. .G.L.....N ....Y 133
cat              GHS.AES.E. ..EPPARVLA PHDN..RA.. RLG.S..M.D .R....RL.. .G.L.....N ..... 132
Mouse            DQGL.----- -KEHPKRVLR SQGST.RVQQ R.QNS.VTHI .S...H.I... .G.V.R...N A.KLL 121
```

Fig. 2 – Alignment of deduced amino acid sequences of Japanese and cynomologus monkeys prepro-BNP with those of human, sheep, pig, camel, cat, and mouse. Dots (···) showing identical amino acids, and dashes (- - -) showing gaps. The GenBank accession numbers are: human (BC025785), sheep (AF037466), pig (NM_213846), camel (AB127392), cat (NM_001009244), and mouse (NM_008726).

script III (Invitrogen). Polymerase chain reaction (PCR) amplification of cDNA was carried out using BNP primers. The primers were 5′-AGCCTCCGCAGTCCCTCCAGAGAC (sense), and 5′-AGGTGTCTGCAGCCAGGACTTCCT (antisense). The amplication profile was the same as used for cloning.

2.4. *Immunospot test*

Human BNP was purchased form Peptide Insitute (Osaka, Japan) and monkey BNP was synthesized by the Central Research Laboratory at Shiga University of Medical Science. Small drops (1 μl) of human and monkey BNP were spotted on the nitrocellulose membrane at a dose of 100, 25, 6.3, 1.2, and 0.4 pmol/μl. After drying in air, the membrane was incubated with 2% gelatin in Tris-buffered saline (pH 7.5) containing 0.1% Tween 20 (TBST) to block non-specific protein binding (Sigma). The membrane was incubated for 2 h with the BNP antibody at 1/5000 dilution in TBST. After washing with TBST, the membrane was incubated for 1 h with a peroxidase-coupled anti-rabbit IgG Fab' fragment (Histofine; Nichirei Corporation, Tokyo, Japan; diluted 1:20). Peroxidase labeling was detected with 0.02% 3,3′-diaminobenzidine in 50 mM Tris–HCl buffer (pH 7.6) containing 0.3% nickel ammonium sulfate.

2.5. *Immunohistochemistry*

Serial cryostat sections (18 μm) were floated in 0.1 M phosphate buffer saline with 0.3% Triton X-100, pH 7.4 (PBST) for 4 days at 4 °C and treated in a free-floating state. Endogenous peroxidase activity was killed by incubation in 0.5% H_2O_2 in PBST, pH 7.4 for 30 min. After rinsing three times with PBST for 10 min each, the sections were incubated in 2% normal goat serum (Invitrogen) for 30 min at room temperature. Then they were incubated for 48 h at 4 °C with a rabbit polyclonal antibody against human-BNP (A-018, IBL Co. Ltd., Gunma, Japan) at a dilution of 1:5000 and polyclonal rabbit antiserum prepared against human-AVP (Chemicon, Temecula, CA, USA), at a dilution of 1:10,000. After rinsing three times with PBST for 10 min each, sections were incubated for 1 h at room temperature with biotinylated goat anti-rabbit IgG at a dilution of 1:500 (Vector Laboratories, Burlingame, CA, USA), then incubated for 1 h at room temperature with an avidin–biotin–peroxidase complex at a dilution of 1:4000 (ABC Elite, Vector Laboratories). The peroxidase-labeled sections were developed in 0.02% 3,3-diamine-benzidine tetrahydrochloride with 0.07% nickel ammonium sulfate in 50 mM Tris–HCl, pH 7.6, with 0.005% hydrogen peroxide.

Double immuostaining was employed to detemine a cell type of BNP-containing cells. After the first BNP immunostaining with purple color, the sections were treated for 30 min at room temperature with 0.5% hydrogen peroxide in PBST to eliminate the residual horseradish peroxidase activity.

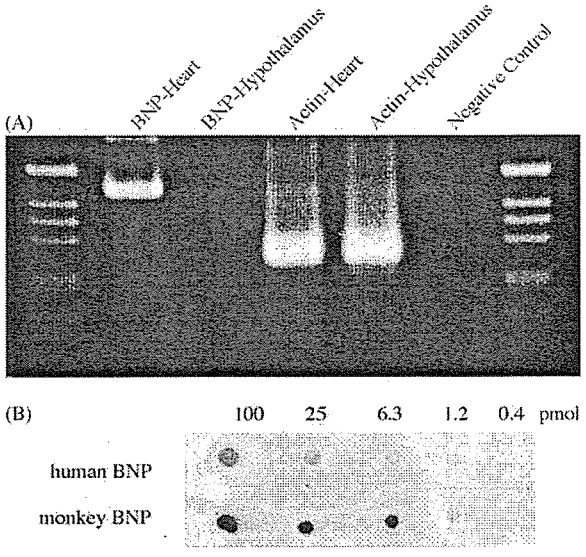

Fig. 3 – (A) Reverse transcription polymerase chain reaction (RT-PCR) analysis for BNP and actin expression in cardiomyocytes and hypothalamus of cynomologus monkey. (B) Immunospot test using human and monkey BNP probed with the BNP antibody (1:5000).

Subsequently, the sections were washed in PBST and incubated with the antibodies to cell markers. The antibodies were mouse monoclonal anti-MAP2 (1:500, Sigma), mouse monoclonal anti-GFAP (1:500, Chemicon), mouse monoclonal anti-CNPase (1:2000, Chemicon), or mouse monoclonal anti-CD54/ICAM-1 (1:100, Immunotech, France) antibodies. After rinsing sections three times with PBST, they were incubated for 2 h at room temperature with histofine anti-mouse IgG complex at a dilution of 1:20 (Nichirei, Japan). Washing three times with PBST, then the sections were developed in 0.02% 3,3-diamine-benzidine tetrahydrochloride in 50 mM Tris–HCl, pH 7.6, with 0.005% hydrogen peroxide to yield a brown color.

For an immunohistochemical control, the sections were stained using the BNP primary antibody pre-absorbed with BNP antigen (human BNP-32 hormone, Peptide Institute, Osaka, Japan) for 24 h at 4 °C. The staining was abolished using the antibody pre-absorbed with BNP peptides (data not shown).

3. Results

3.1. *Molecular cloning of BNP*

Fig. 1 shows the entire coding region of BNP in Japanese and cynomologus monkeys. The nucleotide sequence of Japanese monkey BNP was identical to that of cynomologus monkey except one nucleotide which was T in Japanese monkey prepro-BNP and replaced by C in cynomologus monkey (Fig. 1). But the deduced amino acid sequence was completely identical without any difference (Fig. 2). Prepro-BNP of

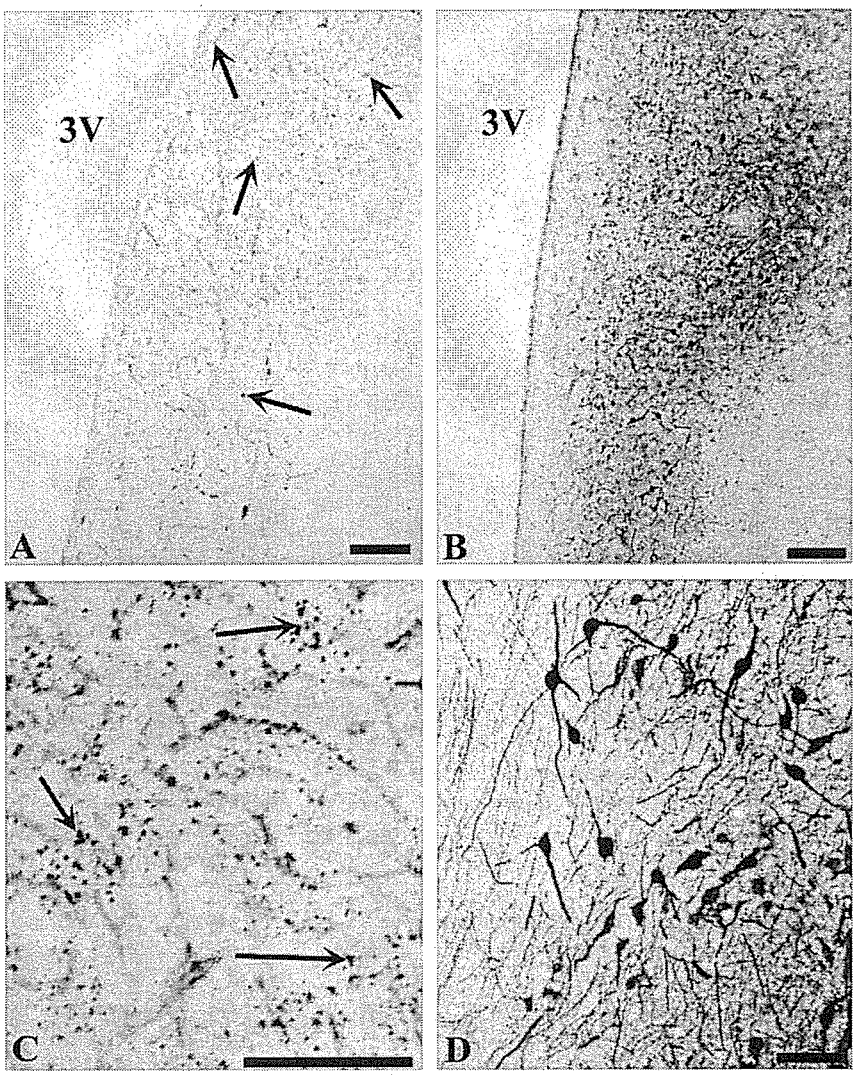

Fig. 4 – (A–D) BNP- and AVP-like immunoreactivity in PVN and periventricular nucleus of cynomologus monkey. (A) BNP-like immunoreactivity in the PVN and periventricular nucleus (arrow). (B) AVP immunoreactivity in the PVN. 3V, third ventricle. (C) High magnification showing BNP immunoreactive clustered granules (arrow). (D) High magnification showing immunoreative vasopressinergic neurons and its neuronal processes in the PVN. Note bipolar and multipolar AVP neurons, and large and small AVP neurons. Bars in (A and B) = 10 μm and (C and D) = 5 μm.

Japanese and cynomologus monkey consisted of 132 amino acid residues (Fig. 2). The signal peptides were 26 amino acid residues, followed by 106 amino acids as pro-BNP which was cleaved into C-terminal 32 amino acid residues and a 74 amino acid N-terminal fragment (Fig. 2). The C-terminal 32 residues which constituted a mature BNP, was preceded by a single arginine residue which is proteolytic processing site. The C-terminal sequence of BNP contained two cysteine residues to form a 17-residue ring structure, which commonly occurs in the natriuretic peptide family (Fig. 2).

The deduced amino acid sequences of prepro-BNP of Japanese and cynomologus monkey were 91% homologous to that of human prepro-BNP which became 97% identical in the mature region (BNP-32). By contrast, it was 54, 52, 51.8, 50.7, and 28% to those of sheep, porcine, camel, cat, and mouse prepro-BNP, respectively (Fig. 2).

3.2. *RT-PCR examination*

RT-PCR analysis showed negative BNP gene in the hypothalamus of cynomologus monkey, although 406 bp of BNP gene was obtained in the heart of cynomologus monkey (Fig. 3A).

3.3. *Immunohistochemical localization of BNP in the hypothalamus*

In order to clarify that the antibody can detect monkey BNP, the immunospot test was employed. The spot test clearly showed that the antibody detected at least 1.2 pmol of both human and monkey BNP (Fig. 3B). Using this antibody, we examined the distribution of BNP-like immunoreactivity in the hypothalamus of cynomologus monkey (Figs. 4A–C and 5A–C).

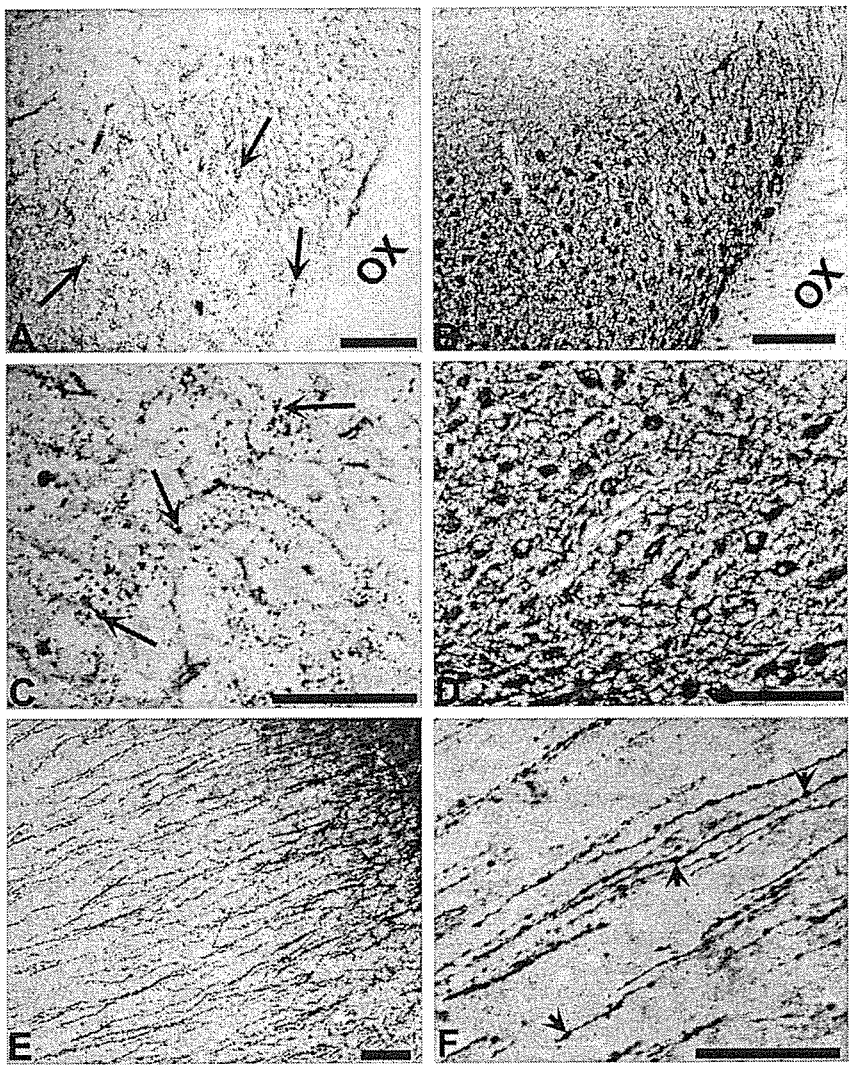

Fig. 5 – (A–D) BNP- and AVP-like immunoreactivity in SON of cynomologus monkey. OX indicates optic chiasma. (A) BNP-like immunoreactivity in the SON. (B) AVP-immunoreativity in the SON. (C) High magnification showing BNP-immunoreactive clusters in the SON (arrow). (D) High magnification showing AVP neurons in the SON. (E and F) The AVP-immunoreactive fibers in the area between the SON and PVN. The AVP-immunoreactive fibers showing varicosities along the fibers (arrow head). Bars in (A, B, and E) = 10 μm and (C, D, and F) = 5 μm.

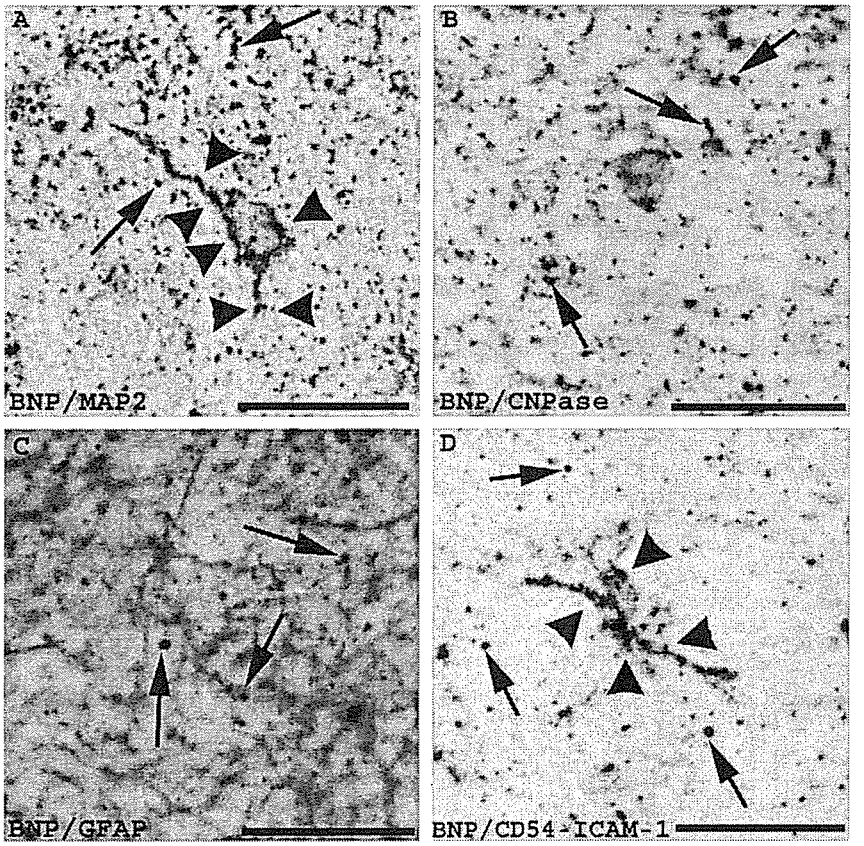

Fig. 6 – Double immunostaining of BNP with cell markers. (A) Many BNP granules distribute among cells (arrows), and some BNP dots are seen surrounding MAP2-positve neurons (arrowheads). (B) BNP granules are seen among CNPase-positive oligodentrocyte (arrows). (C) BNP granules are seen among GFAP-positive astrocytes (arrows). (D) Many BNP granules distribute among cells (arrows), and some BNP dots are seen in CD54/ICAM-1-positve microglia (arrowheads). Bars = 10 μm.

For a comparison, AVP-like immunoreactive neurons were also stained using the adjacent or nearby sections (Figs. 4B–D and 5B–D). BNP-like immunoreactivity was found in the PVN and periventricular area (Fig. 4A–C) as well as the SON (Fig. 5A–C) in the hypothalamus. These areas contain many AVP-positive neuronal perikarya (Figs. 4B–D and 5B–D). However, there are apparent differences of immunopositive structures between BNP and AVP. BNP-like immunoreactivity appeared in the form of clusters of immunoreactive granules. These clusters were particularly dense in the SON. There were no obvious differences in the sizes of BNP-immunoreactive granules between the PVN and SON (Figs. 4A–C and 5A–C). AVP-immunoreacitvity was detected to neuronal perikarya (Figs. 4D and 5D) and varicose fibers (Fig. 4D–F). BNP-like immunoreacitive dots were localized to the PVN, SON and periventricular nucleus. While, AVP-positive varicose fibers were extended from PVN and SON to the medial eminence (Fig. 5E and F).

Double immunostaining showed that some BNP-positive dots appeared to be localized to the surface of MAP-positive neurons (arrowheads in Fig. 6A). Few BNP-positive dots were seen in CNPase-positive oligodendrocyte (Fig. 6B) or GFAP-positive astrocytes (Fig. 6C). Some BNP-positive dots were seen in CD54/ICAM-1-positive microglia (Fig. 6D).

4. Discussion

In the present study, we have cloned and sequenced cDNA encoding Japanese and cynomologus monkeys BNP from cardiac ventricles. The deduced amino acid sequence for monkey prepro-BNP comprised 132 amino acid residues, pro-BNP comprised 106 amino acid residues and the mature BNP comprised 32 amino acid residues. The comparison with human BNP revealed a high degree of identity (91% in prepro-BNP, and 97% in the mature region). Based on the comparison of prepro-BNP sequences of different species, human and monkey were distinct and formed sequences which are independent from other species.

The present study first demonstrated the localization of BNP-like immunoreactivity in the monkey hypothalamus. For immunohistochemical staining of BNP, we used polyclonal anti-human BNP antibody (against BNP-32). Because our monkey BNP cloning data showed very high identity in the

mature region (BNP 32). To verify the specificity of the BNP reaction, we performed "absorption test" which showed no reaction of the BNP antibody pre-absorbed with human BNP.

In the monkey hypothalamus, BNP-immunoreactivity was localized to some granules in the periventricular nucleus as well as the PVN and SON where many AVP-positive neurons existed. Previous studies reported a few BNP-immunoreactivity in these areas of the rat hypothalamus [21]. Some species differences may exist. RT-PCR results showed negative BNP mRNA in the hypothalamus of monkey. The results are supported by a previous study showing that there is no BNP mRNA in the brain [12]. These results suggest that BNP granules in the hypothalamus are originated from outside the hypothalamus. Since BNP and NPR-A were detected in the circumventricular organs such as the subfornical organ [3,13,21], BNP expressed in the heart may reach the hypothalamus through the subfornical organ.

Double immunostaining demonstrated that most BNP-positive granules distributed among cells. Few BNP-positive dots were seen in oligodendrocytes and astrocytes but some were observed in the surface of MAP2-positive neurons. The results suggest that BNP may bind some receptors of neurons. The hypothesis may be supported by the previous studies showing that ANP and BNP inhibit AVP neurons via GC-A receptor [26]. In addition, microglia seem to uptake BNP peptides.

The functional meaning of BNP in monkey hypothalamus remains unclear in this study. However, some possibilities are raised, because of the localization of BNP in area where AVP is highly expressed. Previous studies demonstrated that intracerebroventricular injection of BNP had inhibitory effect on the AVP secretion in hypothalamus [25] or on the stress-induced corticotropin release [7]. In addition, natriuretic peptides inhibited the AVP-induced water permeability of the collecting tubules in rabbit kidney [4] or plasma corticotrophin. Injection of AVP in rats increases plasma immunoreactive BNP concentration [5]. Taken together, the localization of BNP in monkey hypothalamus suggests that BNP may have a central role in modulation of cardiovascular homeostasis through the inhibitory effect on the release of AVP in the hypothalamus.

Acknowledgment

We thank the members of pharmacology department, Shiga University of Medical Science (Japan), for helping us to get the samples.

REFERENCES

[1] Aitken GD, Raizis AM, Yandle TG, George PM, Espiner EA, Cameron VA. The characterization of ovine genes for atrial, brain, and C-type natriuretic peptides. Domest Anim Endocrinol 1999;16:115–21.
[2] Asano K, Murakami M, Endo D, Kimura T, Fujinaga T. Complementary DNA cloning, tissue distribution, and synthesis of canine brain natriuretic peptide. Am J Vet Res 1999;60:860–4.
[3] Brown J, Czarnecki A. Autoradiographic localization of atrial and brain natriuretic peptide receptors in rat brain. Am J Physiol 1990;268:R57–63.
[4] Dilliingham MA, Anderson RJ. Inhibtion of vasopressin action by natriuretic peptide factor. Science 1986;231:1572–3.
[5] Horio T, Kohno M, Takeda T. Effect of arginine vasopressin, angiotensin II and endothelin-1 on the release of brain natriuretic peptidein vivo and in vitro. Clin Exp Pharmacol Physiol 1992;8:575–82.
[6] Itoh H, Nakao K, Saito Y, Yamada T, Shirakami G, Mukoyama M, et al. Radioimmunoassay for brain natriuretic peptide (BNP)-detection of BNP in canine brain. Biochem Biophys Res Commun 1989;158:120–8.
[7] Jaszberenyi M, Bujdoso E, Telegdy G. Effects of brain natriuretic peptide on pituitary–adrenal activation in rats. Life Sci 2000;66(17):1655–61.
[8] Kambayashi Y, Nakao K, Mukoyama M, Saito Y, Ogawa Y, Shiono S, et al. Isolation and sequence determination of human brain natriuretic peptide in human atrium. FEBS Lett 1990;259:341–5.
[9] Kelly R, Struthers AD. Are natriuretic peptides clinically useful as markers of heart failure? Ann Clin Biochem 2001;38:94–102.
[10] Kojima M, Minamino N, Kangawa K, Matsuo H. Cloning and sequence analysis of cDNA encoding a precursor for rat brain natriuretic peptide. Biochem Biophys Res Commun 1989;159:1420–6.
[11] Koller KJ, Goeddel DV. Molecular biology of the natriuretic peptides and their receptors. Circulation 1992;86:1081–8.
[12] Langub Jr MC, Watson Jr RE, Herman JP. Distribution of natriuretic peptide precursor mRNAs in the rat brain. J Comp Neurol 1995;356:183–99.
[13] Langub Jr MC, Dolgas CM, Watson Jr RE, Herman JP. The C-type natriuretic peptide receptor is the predominant natriuretic peptide receptor mRNA expressed in rat hypothalamus. J Neuroendocrinol 1995;7:305–9.
[14] Liu ZL, Wiedmeyer CE, Sisson DD, Solter PF. Cloning and characterization of feline brain natriuretic peptide. Gene 2002;292:183–90.
[15] Minamino N, Aburaya M, Ueda S, Kangawa K, Matsuo H. The presence of brain natriuretic peptide of 12,000 daltons in porcine heart. Biochem Biophys Res Commun 1988;155:470–746.
[16] Nakayama T. The genetic contribution of the natriuretic peptide system to cardiovascular diseases. Endocr J 2005;52:11–21.
[17] Ogawa Y, Itoh H, Nakao K. Molecular biology and biochemistry of natriuretic peptide family. Clin Exp Pharmacol Physiol 1995;22:49–53.
[18] Ogawa Y, Itoh H, Tamura N, Suga S, Yoshimasa T, Uehira M, et al. Molecular cloning of complementary DNA and gene that encode mouse brain natriuretic peptide and generation of transgenic mice that overexpress the brain natriuretic peptide gene. J Clin Invest 1994;93:1911–21.
[19] Osman AH, Yuge S, Hyodo S, Sato S, Maeda S, Marie H, et al. Molecular identification and immunohistochemical localization of atrial natriuretic peptide in the heart of the dromedary camel (*Camelus dromedaries*). Comp Biochem Physiol A Mol Integr Physiol 2004;139:417–24.
[20] Pandey KN. Biology of natriuretic peptides and their receptors. Peptides 2005;26:901–32.
[21] Saper CB, Hurley KM, Moga MM, Holmes RH, Adams SA, Leahy KM, et al. Brain natriuretic peptides: differential localization of a new family of neuropeptides. Neurosci Lett 1989;96:29–34.
[22] Seilhamer JJ, Arfsten A, Miller JA, Lundquist P, Scarborough RM, Lewicki JA, et al. Human and canine gene homologs of porcine brain natriuretic peptide. Biochem Biophys Res Commun 1989;165:650–8.

[23] Sudoh T, Minamino N, Kangawa K, Matsuo H. Brain natriuretic peptide-32: N-terminal six amino acid extended form of brain natriuretic peptide identified in porcine brain. Biochem Biophys Res Commun 1988;155:726–32.
[24] Ueda S, Minamino N, Sudoh T, Kangawa K, Matsuo H. Regional distribution of immunoreactive brain natriuretic peptide in porcine brain and spinal cord. Biochem Biophys Res Commun 1988;155:733–9.
[25] Yamada T, Nakao K, Itoh H, Shirakami G, Kangawa K, Minamino N, et al. Intracerebroventricular injection of brain natriuretic peptide inhibits vasopressin secretion in conscious rats. Neurosci Lett 1988;95:223–8.
[26] Yamamoto S, Inenaga K, Eto S, Yamashita H. Cardiovascular related peptides influence hypothalamic neurons involved in control of body water homeostasis. Obes Res 1995;5:789–94.

ELSEVIER

Stable Maintenance of Monkey Embryonic Stem Cells in the Absence of bFGF

A. Yamashita, T. Takada, G. Yamamoto, and R. Torii

ABSTRACT

Monkey embryonic stem (ES) cells are useful tools in preclinical studies of gene therapy and tissue engineering as well as in primate developmental biology. However, their maintenance is not easy, requiring addition of bFGF to the medium.[1] Herein, we have described a stable, cost-effective method that does not require bFGF. We used a high-density (1 to 1.5 $\times$ 10^5 cells/cm^2) of mouse embryonic fibroblasts (MEF) as feeder cells to successfully maintain undifferentiated monkey ES cells for 2 years (~150 passages). Furthermore, these ES cells were competent for electroporation of enhanced green fluorescent protein (EGFP) and subsequent drug selection procedures. We were able to establish EGFP-expressing cell lines using this culture condition. These cell lines expressed undifferentiated markers, such as alkaline phosphatase, SSEA-4, TRA-60, and TRA-81. In addition, strong EGFP expression was observed after differentiation into cardiomyocytes, neurons, or adipocytes, suggesting that these cell lines are a useful tool to study cell transplantation.[1,2] This method simplifies the culture of monkey ES cells.

NONHUMAN PRIMATE embryonic stem (ES) cells are considered to be one of the best models to study human development and stem cell therapy. However, monkey ES cell cultures are more complicated and difficult than those of mouse ES cells. For example, the addition of bFGF has been required to maintain their undifferentiated state.[1] Because recombinant bFGF is expensive and labile, this requirement hinders the use of monkey ES cells. Herein, we sought to culture monkey cells stably in the absence of bFGF. We succeeded in establishing EGFP-expressing monkey ES cell lines by electroporation under this culture condition.

MATERIALS AND METHODS

Cynomolgus monkey ES cells (CMS-A2) were maintained on a mitomycin C inactivated feeder layer of neomycin-resistant MEF in DMEM/F12 medium (Sigma, St. Louis, Mo, USA), containing 20% knockout serum replacement (KSR; Invitrogen, Carlsbad Calif, USA), 100 μmol/L 2-mercaptoethanol (Sigma), 1% nonessential amino acids (Sigma), 1 mmol/L Na pyruvate (Sigma), and 2 mmol/L L-glutamine (Sigma) in a humidified 5% CO_2 atmosphere at 37 °C.[3] The medium was changed daily. A high-density MEF layer (1 to 1.5 $\times$ 10^5 cells/cm^2) was prepared in a 0.1% gelatin-coated dish.

For transfection experiments, we constructed an EGFP vector (pEGFP-1, Clontech, Palo Alto, Calif) under the control of the CAG promoter[4] (a gift from J. Miyazaki). Forty micrograms of linealized vector was electroporated into a suspension of ES cells (10^7 cells) in 0.8 mL of PBS using a Bio-Rad gene pulser (500 μF, 250 V).[2] Cells were incubated on ice for 10 minutes, plated, and allowed to recover for 48 hours before selection with G418 (100 μg/mL). Cells were fed daily for 10 days, whereafter, the resulting G418-resustant ES colonies showing strong EGFP expression were individually picked and propagated. To analyze stem cell markers, alkaline phosphatase activity and cell surface markers were detected using an ES cell characterization kit (Chemicon, Temecula, Calif).

RESULTS AND DISCUSSION

We maintained monkey ES cells in an undifferentiated state in the absence of bFGF for 2 years (~150 passages) and to establish undifferentiated EGFP-expressing ES cell lines (Fig 1) by electroporation.[1,2] In contrast, less than 4 $\times$ 10^4 cells/cm^2 (8 $\times$ 10^5 cells/6 cm dish) of MEF did not maintain undifferentiated monkey ES cells in the absence of exogenous bFGF. We found that 1 to 1.5 $\times$ 10^5 cells/cm^2 MEF density gave the best results for maintenance of the undif-

From the Research Center for Animal Life Science (A.Y., T.T., R.T.) and the Department of Oral and Maxillofacial Surgery (A.Y., G.Y.), Shiga University of Medical Science, Ohtsu, Japan.

Address reprint requests to T. Takada, Research Center for Animal Life Science, Shiga University of Medical Science, Tsukinowa-cho, Seta, Ohtsu 520-2192 Japan. E-mail: ttakada@belle.shiga-med.ac.jp

0041-1345/06/$–see front matter
doi:10.1016/j.transproceed.2006.02.059

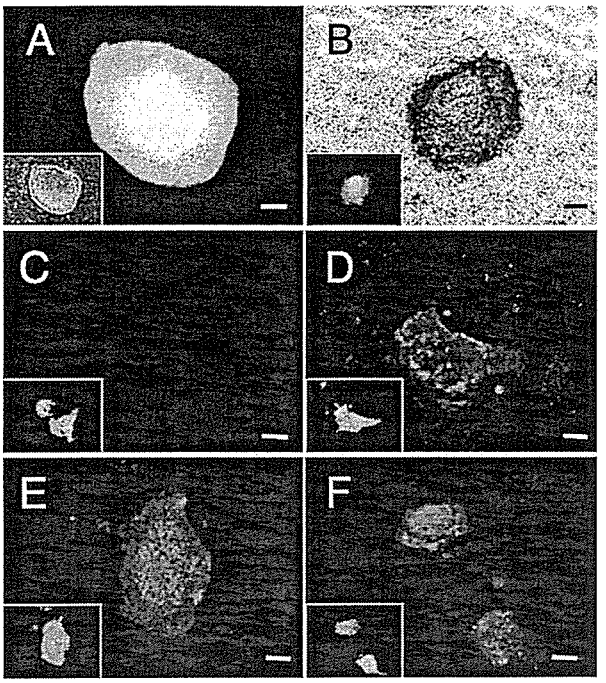

Fig 1. Cynomolgus monkey ES clone stablely expressing EGFP **(A)**. Expression of the markers: alkaline phosphatase **(B)**, SSEA-1 **(C)**, SSEA-4 **(D)**, TRA-60 **(E)**, and TRA-81 **(F)**. Insets are bright field image **(A)** and EGFP fluorescent images **(B, C, D, E, F)**. Scale bars = 100 μm.

ferentiated state. Recently, Wang et al[5] reported that MEF expressed bFGF and noggin, which play an important role to maintain the undifferentiated state of human ES cells.[5] Normally, 4 to 10 ng/mL of bFGF was added into the medium. Therefore, equivalent levels of bFGF or other growth factors as well as exracellular matrix are provided by high-density MEF. As they grow under these culture conditions, ES cells form tightly packed domed colonies (Fig 1A). No significant differences in morphology and marker expression were observed between untransfected and transfected ES cells (data not shown). These results imply that high-density MEF enabled us to maintain monkey ES cells in the absence of bFGF and even supported the proliferation of damaged ES cells after electroporation. These cells maintained EGFP expression after differentiation into cardiomyocytes, neurons, or adipocyte (data not shown), suggesting that this cell line may be a useful tool for tracing grafted cells in transplantation studies.

As the method totally relies on MEF for secreted factors and extracellular matrix, it is important to use early passage (less than P-4) of MEF and care should be taken about the quality of MEF to maintain an undifferentiated state. This high-density MEF culture has another advantage: ES cells can be easily separated from MEF feeders by collagenase treatment. Undifferentiated ES cells come off with collagenase, while the MEF layer remain attached forming a sheet, which is beneficial for passage, electroporation, and embryoid body formation, because it is important to minimize contamination of MEF in these procedures. Therefore, the high-density MEF culture simplifies not only ES cell cultures but also subsequent experimental procedures required in stem cell biology.

REFERENCES

1. Furuya M, Yasuchika K, Mizutani K, et al: Electroporation of cynomolgus monkey embryonic stem cells. Genesis 37:180, 2003

2. Takada T, Suzuki Y, Kondo Y, et al: Monkey embryonic stem cell lines expressing green fluorescent protein. Cell Transplant 11:631, 2002

3. Yamashita A, Takada T, Narita J, et al: Osteoblastic differentiation of monkey embryonic stem cells in vitro. Cloning Stem Cells 7:232, 2005

4. Niwa H, Yamamura K, Miyazaki J: Efficient selection for high-expression transformants with novel eukaryotic vector. Gene 108:193, 1991

5. Wang G, Zang H, Zhao Y, et al: Noggin and bFGF cooperate to maintain the pluripotency of human embryonic stem cells in the absence of feeder layers. Biochem Biophys Res Commn 330:934, 2005

FEBS Letters 580 (2006) 4121–4125

Transient suppression of PPARγ directed ES cells into an osteoblastic lineage

Akihiro Yamashita[a,b], Tatsuyuki Takada[a,*], Ken-ichi Nemoto[a], Gaku Yamamoto[b], Ryuzo Torii[a]

[a] *Research Center for Animal Life Science, Shiga University of Medical Science, Tsukinowa-cho, Seta, Ohtsu 520-2192, Japan*
[b] *Department of Oral and Maxillofacial Surgery, Shiga University of Medical Science, Tsukinowa-cho, Seta, Ohtsu 520-2192, Japan*

Received 2 April 2006; revised 2 June 2006; accepted 20 June 2006

Available online 30 June 2006

Edited by Ned Mantei

Abstract Osteoblasts and adipocytes are believed to share a common progenitor. Peroxisome proliferator-activated receptor γ (PPARγ) plays a key role in the switching of these two cell lineages. Here, we demonstrated the differentiation of ES cells into an osteoblastic lineage using siRNA against PPARγ without the addition of any osteogenic factors. We found that PPARγ-siRNA downregulated the expression of aP2 mRNA and lipid accumulation, whereas it upregulated the expression of osteocalcin and calcium deposition. These results suggested that ES cells were directed into an osteoblastic lineage. Therefore, transient suppression using PPARγ-siRNA may be a novel tool to induce differentiation of ES cells into osteoblasts.

Keywords: ES cell; Small interfering RNA; Peroxisome proliferator-activated receptor γ; Osteogenesis; Adipogenesis

1. Introduction

Production of various functional cells from ES cells is a critical issue for regenerative medicine. The differentiation of ES cells into osteoblasts has been achieved using a combination of retinoic acid (RA), ascorbic acid, β-glycerophosphate, dexamethasone (Dex), and bone morphogenetic protein-2 (BMP-2) [1–4,24].

Interestingly, it has been reported that osteoblasts and adipocytes share common progenitors in the bone marrow and their relationship with regard to differentiation is reciprocal [5,6]. In addition, clinical evidence that a decrease in bone volume of age-related osteoporosis is accompanied by an increase in marrow adipose tissue also implies the possible reciprocal relationship of these lineages [7,8].

PPARγ is a transcription factor abundantly expressed in adipose tissue and plays a key role in adipocyte differentiation, insulin sensitivity and immune responses [9]. The biological role of PPARγ had been investigated by using PPARγ-deficient mice generated by gene targeting [9]. The heterozygous PPARγ-deficient (PPARγ+/−) mice exhibited resistance to high-fat diet-induced obesity and insulin resistance [9,10]. This PPARγ insufficiency enhanced osteogenesis from bone marrow progenitors in vivo and ex vivo [11].

Furthermore, homozygous PPARγ-deficient (PPARγ−/−) ES cells were unable to differentiate into adipocytes and spontaneously differentiated into osteoblasts [11]. This evidence suggested that PPARγ plays a key role in switching the commitment of the common progenitor into either adipocytic or osteoblastic lineages in bone marrow. Therefore, we considered that osteoblasts might also be induced from differentiated ES cells by suppressing PPARγ.

Recently, RNA interference (RNAi) has become a powerful tool for selectively silencing the expression of the target gene [12]. We have established an efficient method to suppress specific genes using chemically synthesized siRNA in ES cells [13]. Modulating the cell fate by suppressing the expression of a key gene using siRNA has the great advantage that the effect is transient and does not jeopardize the genome organization. Therefore, the use of siRNA will be an ideal differentiation method for regenerative medicine and could be applied to the adult stem cells to induce the desired cell types.

In this paper, we attempted to develop a novel method to differentiate ES cells into an osteoblastic lineage by transiently suppressing a key transcription factor PPARγ using synthetic siRNA. We show that siRNA against PPARγ suppressed adipocyte differentiation and successfully induced osteoblastic differentiation in ES cells without using factors such as ascorbic acid, β-glycerophosphate, Dex and BMP-2, which are known to promote osteogenesis.

2. Materials and methods

2.1. Mouse ES cell culture and differentiation

Mouse ES cells (SV6) were cultured with DMEM containing 15% FCS, 0.1 mM 2-mercaptoethanol and 1000 U/ml leukemia inhibitory factor (LIF, Invitrogen), as described previously [14]. To initiate differentiation, 1×10^3 cells were cultured with the ES medium without LIF on the inner side of 100 mm culture dish lids and incubated at 37 °C with 5% CO_2. By gravitational force, the cells condensed to form embryoid bodies (EB). After two days of culture, 100 nM all-*trans* RA was added to the medium and the cells were cultured for three more days [15].

Then, EB were washed in PBS and trypsinized, and dissociated cells (1×10^5 cells) were plated at 1×10^5 cells/ml onto a 35 mm culture dish coated with 0.1% gelatin. Cells were cultivated using ES medium without LIF.

For positive control of osteoblast and adipocyte differentiation, cells were induced to differentiate using osteogenic supplements (OS: 50 μg/ml ascorbic acid, 10 mM β-glycerophosphate, 100 nM Dex) and adipogenic supplements (AS: 0.5 mM 3-isobutyl-L-methylxanthine, 250 nM Dex, and 100 nM insulin) as described previously [4,23].

*Corresponding author. Fax: +81 77 548 2414.
E-mail address: ttakada@belle.shiga-med.ac.jp (T. Takada).

0014-5793/$32.00
doi:10.1016/j.febslet.2006.06.057

2.2. siRNA transfection

We selected siRNAs corresponding to a conserved sequence (nucleotides 320–344; Accession No. NM_011146) to target transcripts of the mouse PPARγ gene (annealed oligos 5′-AAUAUGACCUGAAGCUCCAAGAAUAAG-3′ and 5′-UAUUCUUGGAGCUUCAGGUCAUAUUAU-3′, iGene, Japan). We also used a negative control siRNA, whose sequence does not match any mouse genomic sequence (annealed oligos 5′-AUCCGCGCGAUAGUACGUAdTdT-3′ and 5′-UACGUACUAUCGCGCGGAUdTdT-3′, B-Bridge, Japan). Transfection of siRNA was carried out on the day after the EB plating. The conditions of the RNAi protocol were essentially as described previously [13,16]. Two micro liters of Lipofectamine 2000 (Invitrogen) were mixed with 100 μl of Opti-MEM medium (Invitrogen) and incubated for 5 min at room temperature. Two micro liters of pre-annealed siRNAs (at a concentration of 20 μM) was diluted in 100 μl of Opti-MEM medium, mixed with the diluted Lipofectamine and incubated for another 20 min. The mixture was added to the cells (1 ml of ES medium without LIF in 3.5 cm dish), giving a final concentration of 33 nM RNA in the dish.

2.3. RNA extraction and quantitative reverse transcription-polymerase chain reaction

Total RNA was isolated from the cell culture using an RNeasy Mini Kit (Qiagen) according to the manufacturer's instructions. After DNase treatment of the samples, reverse transcription was carried out using a SuperScript III First-Strand Synthesis System (Invitrogen). Polymerase chain reaction (PCR) reactions (50 μl) were carried out using Blend Taq DNA Polymerase (TOYOBO, Japan) according to the manufacturer's instructions. The PCR conditions used were: 2 min at 94 °C, followed by 35 cycles of 15 s denaturation at 94 °C, 30 s annealing at 55 °C and 30 s extension at 72 °C. Amplified products were used to derive standard curves for quantitative reverse transcription (RT)-PCR. PCR reaction mix for quantitative RT-PCR was prepared using LightCyclerFastStart DNA Master SYBR Green I Kit (Roche). Mg^{2+} concentrations used for the PCR reaction were 3 mM. PCR conditions for quantitative RT-PCR were as follows; activation of enzyme at 95 °C for 10 min, 45 cycles of denaturation at 95 °C for 15 s, annealing at 60 °C for 5 s and extension at 72 °C for 20 s. For PPARγ quantification, SYBR Premix Ex Taq Kit (Takara, Japan) was also used. The condition of quantitative RT-PCR were as follows; activation of enzyme at 95 °C for 10 s, 45 cycles of denaturation at 95 °C for 5 s, annealing at 60 °C for 20 s and extension at 72 °C for 10 s. Quantitative RT-PCR was carried out using the LightCycler Instrument (Roche) and data were analyzed using LightCycler Software Ver.3. Fluorescence of each sample was determined after every cycle. All the melting curves of PCR products gave a single peak with the same melting temperature as the relevant control. Agarose gel electrophoresis of representative reactions was carried out to confirm amplification of unique fragments of predicted lengths. The expressions of marker genes were normalized to the expression of β-actin.

Primer were designed based on the mouse sequence and BLAST-ed for their specificity at the National Center for Biotechnology Information (NCBI). Primer sequences (sense, antisense) were as follows. PPARγ (5′-AAGAGCTGACCCAATGGTTG-3′, 5′-TCCATAGTGGAAGCCTGATGC-3′), adipocyte-specific fatty acid binding protein (aP2) (5′-ATGTGTGATGCCTTTGTGGGA-3′, 5′-TGCCCTTTCATAAACTCTTGT-3′), collagen type 1 (5′-CTGCCTGCTTCGTGTAAA-3′, 5′-ACGTTCAGTTGGTCAAAGGTA-3′), osteopontin (5′-TCTCCTTGCGCCACAGAATG-3′, 5′-TCCTTAGACTCACCGCTCTT-3′), Cbfa1 (5′-CCGCACGACAACCGCACCAT-3′, 5′-CGCTCCGGCCCACAAATCTC-3′), osteocalcin (5′-TCTCTCTGCTCACTCTGCTGG-3′, 5′-ACCGTAGATGCGTTTGTAGGC-3′). β-Actin (5′-GGCCCAGAGCAAGAGAGGTATCC-3′, 5′-ACGCACGATTTCCCTCTCAGC-3′).

2.4. Cell staining

2.4.1. Oil-red O staining and lipid accumulation assay. Lipid accumulation was detected with Oil-red O at 20 days of differentiation, as described previously [17]. For the analysis of lipid accumulation, stained lipid was extracted with 100% isopropanol for 5 min and the optical density of the solution was measured at 540 nm.

2.4.2. Alizarin Red S staining and calcium assay. Calcification was identified with Alizarin Red S staining at 20 days of differentiation [18]. Furthermore, the deposited calcium was extracted with 0.5 M acetic acid over night and the calcium content of the individual dish was determined with the use of the calcium C-test Wako Kit (Wako, Japan), which is based on the *o*-cresolphthalein complexon color development method [19].

2.5. Statistical analysis

Means ± standard deviation (S.D.) were calculated and statistically significant differences between two groups were determined by Student's *t* test at $P < 0.05$.

3. Results and discussion

The expression of PPARγ was induced during the differentiation process in hanging drop culture with RA (Fig. 1A, 5 days). After the adhesion of dissociated EBs, siRNA against PPARγ was transfected to suppress PPARγ expression.

At 10 and 15 days of differentiation in adhesion culture, the expression of PPARγ, which is a marker gene in adipogenesis [20], was significantly suppressed in PPARγ-siRNA-transfected cells, whereas upregulation was observed in cells transfected with control siRNA and cultured with AS (positive control) (Fig. 1A). At 20 days of differentiation, the expression in PPARγ-siRNA-transfected cells was upregulated but still low compared to that of controls (Fig. 1A). Interestingly, the

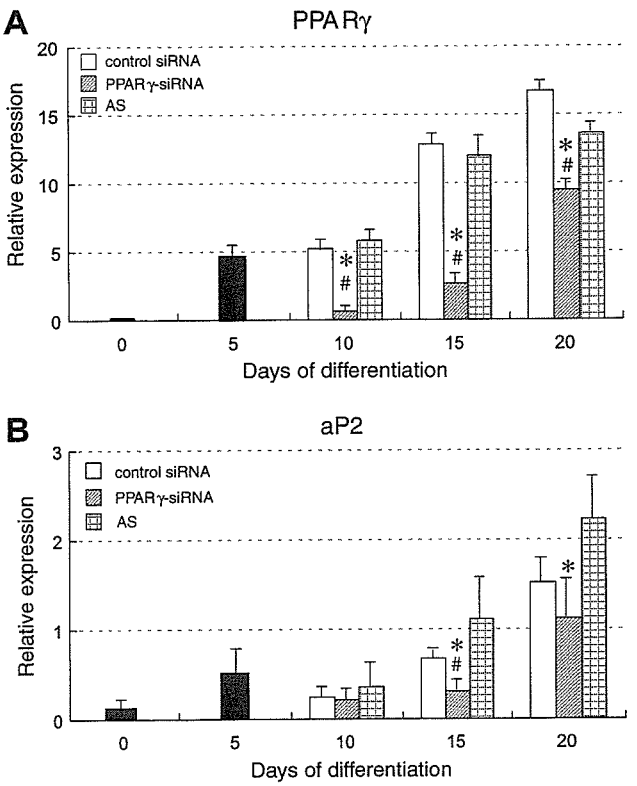

Fig. 1. Expression of marker genes characteristic of adipocytes. Expression of PPARγ (A) and aP2 (B) mRNAs was analyzed by quantitative RT-PCR at 0 days (black bar; undifferentiated mouse ES cells), 5 days (black bar; RA-treated EB), 10 days, 15 days and 20 days of differentiation. Cells transfected with control siRNA, PPARγ-siRNA, or treated with adipogenic supplements (AS) are indicated by open, shaded, and hatched bars, respectively. Data are expressed as means ± S.D. ($n = 3$); # and * indicate significant differences compared to cells transfected with control siRNA or treated with adipogenic supplements, respectively; $P < 0.05$ with Student's *t* test.

expression level of adipocyte-specific fatty acid binding protein (aP2) also remained low in PPARγ-siRNA-transfected cells for 15 days (Fig. 1B). These results indicated that the expression of not only PPARγ, but also of aP2, was successfully downregulated for 15 days by PPARγ-siRNA transfection.

Then, we visualized the lipid accumulation using Oil-red O staining. Control siRNA-transfected cells displayed significant lipid accumulation at 20 days of differentiation (Fig. 2A). In PPARγ-siRNA-transfected cells, the amount of stained lipid was less than that of control siRNA-transfected cells (Fig. 2B). We extracted stained lipid and measured its absorbance to compare lipid accumulation between control and PPARγ-siRNA-transfected cells. Although mouse ES cell eventually become adipocytic even in basic medium under these experimental conditions, a significant reduction of absorbance was observed in PPARγ-siRNA-transfected cells (Fig. 2C). Recently, it has been reported that lentiviral and adenoviral vector-mediated RNAi for PPARγ inhibited preadipocyte to adipocyte differentiation in 3T3-L1 cells [21,22]. Our results demonstrated that the transient suppression of PPARγ using synthetic siRNA inhibited adipocyte differentiation and lipid accumulation per cell in mouse ES cells, suggesting the importance of PPARγ for adipocyte differentiation.

Next, we investigated osteoblast differentiation under the same experimental conditions, except that the positive control cells were cultured with OS. We measured expression of marker genes characteristic of osteoblast differentiation, such as collagen type 1 (COL1), osteopontin (OP), Cbfa1 and osteocalcin (OC). Interestingly, the pattern of COL1 expression in siRNA-transfected cells was different from that of cells cultured with OS (Fig. 3A). COL1 expression was immediately upregulated in OS treated cells. On the other hand, it remained low level for 15 days in siRNA-transfected cells. At 20 days, its expression was upregulated in PPARγ-siRNA transfected cells and reached levels similar to those in the OS treated cells. These results suggest that COL1 expression is differentially affected by OS treatment vs. PPARγ suppression using siRNA. The expression of osteopontin was upregulated by RA treatment, and then was gradually downregulated during the differentiation period. No substantial difference was observed among the culture conditions used (Fig. 3B). On the other hand, expression of Cbfa1 was gradually upregulated by PPARγ-siRNA transfection and a significant difference from control was observed at 15 days (Fig. 3C). In the case of OC, a marker of mature osteoblasts, expression levels did not differ so much in any treatment until 15 days. However, upregulation was detected in PPARγ-siRNA-transfected cells at 20 days of differentiation and the expression level was similar to that in the positive control (Fig. 3D). Furthermore, we examined calcium deposition with Alizalin Red S staining and found obvious staining pattern only in PPARγ-siRNA-transfected cells (Fig. 4). We also measured the amount of accumulated calcium using a colorimetric method [19]. We found that approximately 4 times as much as calcium was accumulated in PPARγ-siRNA-transfected cells compared to control transfected cells, and the amount of accumulated calcium was equivalent to that of OS treated cells at 20 days of differentiation (Fig. 4C). These results demonstrated that the transient suppression of PPARγ promoted osteogenesis. It is notable that we were able to differentiate ES cells into an osteoblastic lineage without adding any osteogenic factors such as ascorbic acid, β-glycerophosphate, Dex or BMPs. This is the first report to our knowledge that osteoblasts were produced from normal ES cells (not PPARγ deficient cells) without using such factors.

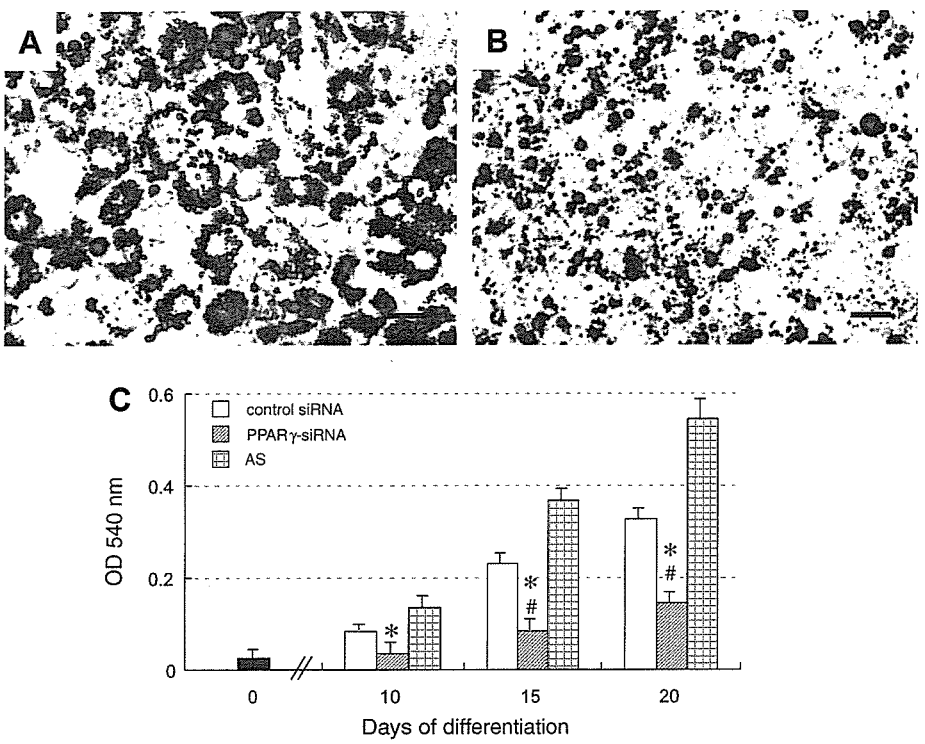

Fig. 2. Effect of PPARγ suppression in adipogenesis. Lipid accumulation was detected by Oil-red O staining at 20 days of differentiation in (A) cells transfected with control siRNA or with (B) PPARγ-siRNA. Scale bar indicates 10 μm. After staining with Oil-red O, stained lipid was extracted and the absorbance at 540 nm was measured (C). Bars as in Fig. 1. Data are expressed as means ± S.D. ($n = 4$) per well; # and * indicate significant differences compared to cells transfected with control siRNA or treated with adipogenic supplements ($P < 0.05$, Student's t test).

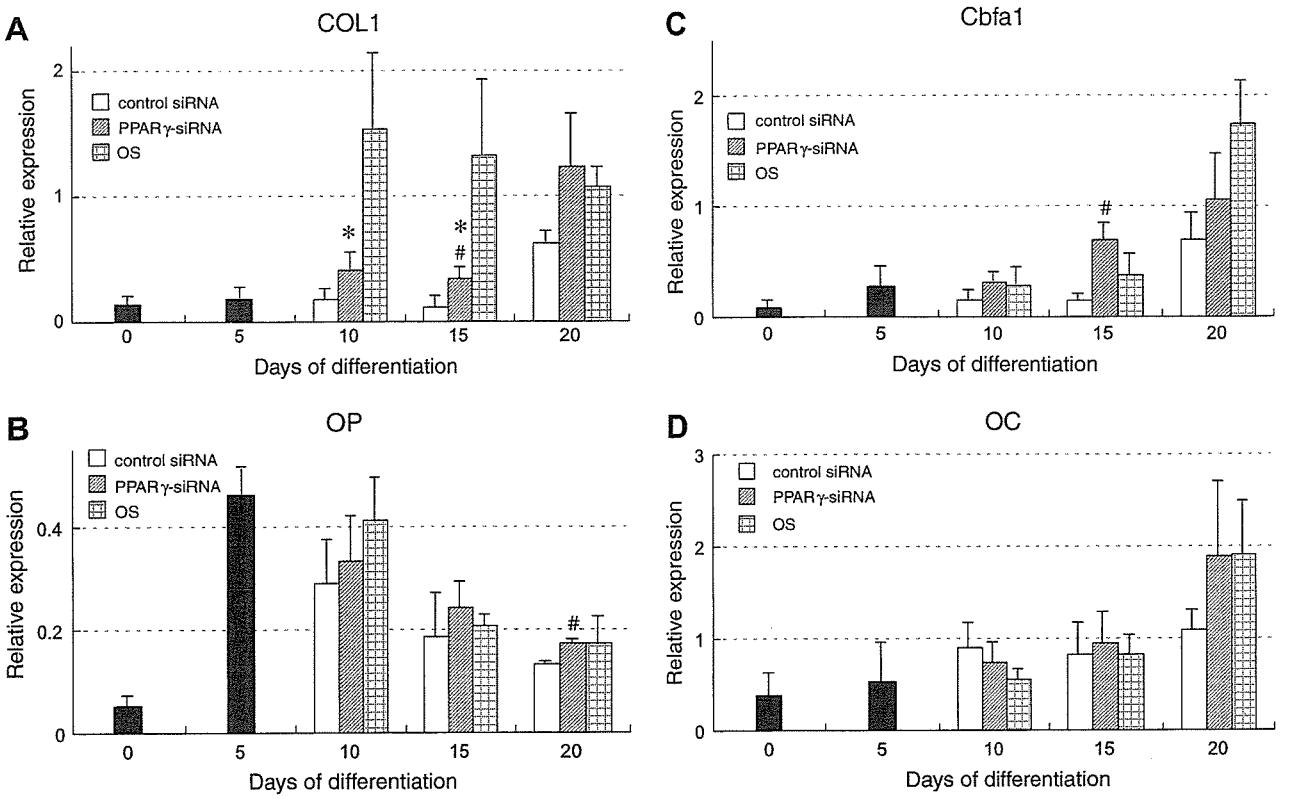

Fig. 3. Expression of marker genes characteristic of osteoblasts. Expressions of collagen type 1 (COL1)(A), osteopontin (OP)(B), Cbfa1 (Cbfa1)(C) and osteocalcin (OC)(D) mRNAs were analyzed with quantitative RT-PCR at 0 day (black bar; undifferentiated mouse ES cells), 5 days (black bar; RA-treated EB), 10 days, 15 days and 20 days of differentiation. Cells transfected with control siRNA, PPARγ-siRNA, or treated with osteogenic supplements (OS) are indicated by open, shaded, and hatched bars, respectively. Data are expressed as means ± S.D. ($n = 3$); # and * indicate significant differences compared to cells transfected with control siRNA or treated with osteogenic supplements ($P < 0.05$, Student's t test).

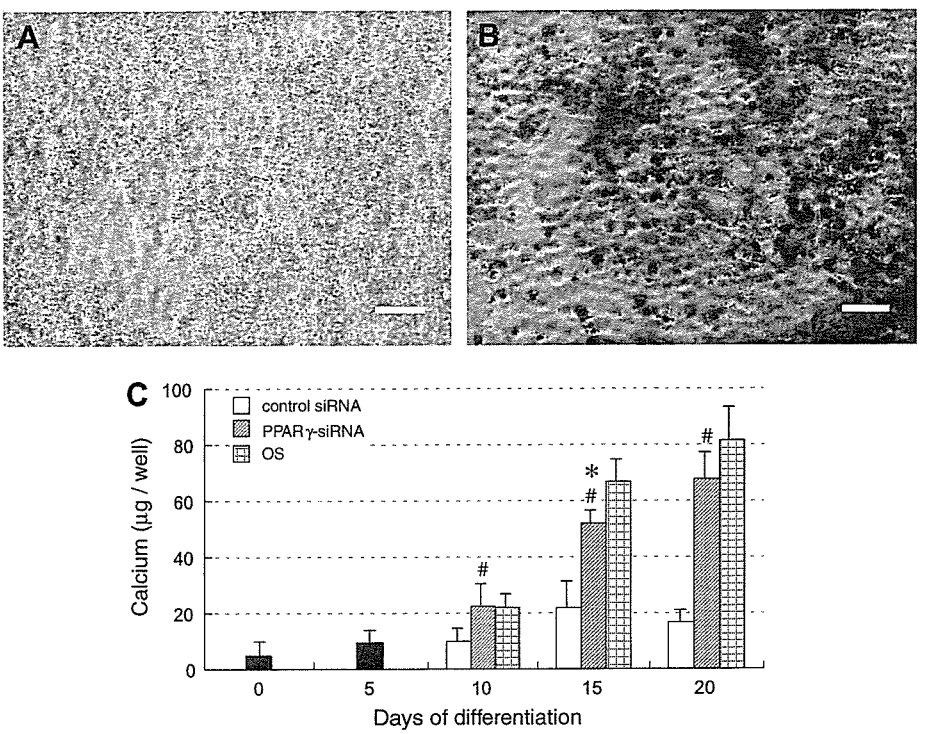

Fig. 4. Effect of PPARγ suppression on osteogenesis. Calcium deposition was detected by Alizarin Red S staining at 20 days of differentiation in cells transfected with control siRNA (A) or PPARγ-siRNA (B). Scale bar indicates 100 μm. Calcium was extracted and quantified by the *o*-cresolphthalein complexon color development method (C). Data are expressed as means ± S.D. ($n = 4$) per well; # and * indicate significant differences compared to cells transfected with control siRNA or treated with osteogenic supplements, respectively ($P < 0.05$, Student's t test).

Here, we showed the transient suppression of PPARγ inhibited adipocyte differentiation, and also induced osteoblast differentiation in ES cells. Our data showed good agreement with the previous observation using PPARγ deficient ES cells [11]. This could be due to the interaction of PPARγ with TGF-β/Smad3 signaling or due to sharing the same progenitors [7,8]. However, the signaling of PPARγ suppression to inhibit adipogenesis and to induce osteogenesis needs to be elucidated further.

Our data suggested that ES cell differentiation could be modified by transient suppression of PPARγ using chemically synthesized siRNA. As synthetic siRNAs have advantages that they are easy to transfect and do not modify genome organization, we believe that this would be an ideal method for cell differentiation for ES, adult stem and progenitor cells.

It is known that osteoblasts and adipocytes develop from common progenitors by the activation of transcription factors Cbfa1 and PPARγ, respectively [11], and age-related osteoporosis is accompanied by an increase in marrow adipose tissue [7,8]. Previous studies have demonstrated that PPARγ acts to promote adipocyte vs. osteoblast differentiation [11]. Our results also support the notion that PPARγ plays an important role in controlling not only adipocyte, but also osteoblast differentiation. In addition, these results suggest the possibility that adipocyte and osteoblast differentiation could be controlled by the transient suppression of PPARγ using siRNA.

In summary, we showed that the transient suppression of PPARγ inhibited adipocyte differentiation and enhanced osteoblast differentiation in ES cells without the use of osteogenic factors. Therefore, cell differentiation using the transient suppression of specific genes with siRNA may provide a novel approach in stem cell biology, regenerative medicine and gene therapy.

Acknowledgements: We thank Y. Kondo for providing mouse ES cells (SV6). This work was supported in part by grants from the Ministry of Education, Science, Sports, and Culture (T.T. and R.T.) and by intramural grants from Shiga University of Medical Science (T.T.).

References

[1] Buttery, L.D., Bourne, S., Xynos, J.D., Wood, H., Hughes, F.j., Hughes, S.P., Episkopou, V. and Polak, J.M. (2001) Differentiation of osteoblasts and in vitro bone formation from murine embryonic stem cells. Tissue Eng. 7, 89–99.

[2] Phillips, B.W., Belmonte, N., Vernochet, C., Ailhaud, G. and Dani, C. (2001) Compactin enhances osteogenesis in murine embryonic stem cells. Biochem. Biophys. Res. Commun. 284, 478–484.

[3] Sottile, V., Thomson, A. and Mcwhir, J. (2003) In vitro osteogenic differentiation of human ES cells. Cloning Stem Cells 5, 149–155.

[4] Yamashita, A., Takada, T., Narita, J., Yamamoto, G. and Torii, R. (2005) Osteoblastic differentiation of monkey embryonic stem cells in vitro. Cloning Stem Cells 7, 232–237.

[5] Nuttall, M.E., Patton, A.J., Olivera, D.L., Nadeau, D.P. and Gowen, M. (1998) Human trabecular bone cells are able to express both osteoblastic and adipocytic phenotype: implications for osteopenic disorders. J. Bone Miner. Res. 13, 371–382.

[6] Beresford, J.N., Bennett, J.H., Devlin, C. and Owen, M.E. (1992) Evidence for an inverse relationship between the differentiation of adipocytic and osteogenic cells in rat marrow stromal cell cultures. J. Cell Sci. 102, 341–351.

[7] Meunier, P., Aaron, J., Edouard, C. and Vignon, G. (1971) Osteoporosis and the replacement of cell populations of the marrow by adipose tissue. A quantitative study of 84 iliac bone biopsies. Clin. Orthop. 80, 147–154.

[8] Rozman, C., Feliu, E., Berga, L., Reverter, J.C., Climent, C. and Ferran, M.J. (1989) Age-related variations of fat tissue fraction in normal human bone marrow depend both on size and number of adipocytes: a stereological study. Exp. Hematol. 17, 34–37.

[9] Kubota, N., Terauchi, Y., Miki, H., Tamemoto, H., Yamauchi, T., Komeda, K., Satoh, S., Nakano, R., Ishii, C., Sugiyama, T., Eto, K., Tsubamoto, Y., Okuno, A., Murakami, K., Sekihara, H., Hasegawa, G., Naito, M., Toyoshima, Y., Tanaka, S., Shiota, K., Kitamura, T., Fujita, T., Ezaki, O., Aizawa, S. and Kadowaki, T., et al. (1999) PPARγ mediates high-fat diet-induced adipocyte hypertrophy and insulin resistance. Mol. Cell 4, 597–609.

[10] Kadowaki, T. (2000) Insights into insulin resistance and type 2 diabetes from knockout mouse models. J. Clin. Invest. 106, 459–465.

[11] Akune, T., Ohba, S., Kamekura, S., Yamaguchi, M., Chung, U.I., Kubota, N., Terauchi, Y., Harada, Y., Azuma, Y., Nakamura, K., Kadowaki, T. and Kawaguchi, H. (2004) PPARγ insufficiency enhances osteogenesis through osteoblast formation from bone marrow progenitors. J. Clin. Invest. 113, 846–855.

[12] Sharp, P.A. (2001) RNA interference-2001. Genes Dev. 15, 485–490.

[13] Takada, T., Nemoto, K., Yamashita, A., Kato, M., Kondo, Y. and Torii, R. (2005) Efficient gene silencing and cell differentiation using siRNA in mouse and monkey ES cells. Biochem. Biophys. Res. Commun. 331, 1039–1044.

[14] Smith, A.G. (1991) Culture and differentiation of embryonic stem cells. J. Tissue Culture Methods 13, 89–94.

[15] Dani, C., Smith, A.G., Dessolin, S., Leroy, P., Staccini, L., Villageois, P., Darimont, C. and Ailhaud, G. (1997) Differentiation of embryonic stem cells into adipocytes in vitro. J. Cell Sci. 110, 1279–1285.

[16] Elbashir, S.M., Harborth, J., Weber, K. and Tuschl, T. (2002) Analysis of gene function in somatic mammalian cells using small interfering RNAs. Methods 26, 199–213.

[17] Ramirez-Zacarias, J.L., Castro-Munozledo, F. and Kuri-Harcuch, W. (1992) Quantitation of adipose conversion and triglycerides by staining intracytoplasmic lipids with Oil red O. Histochemistry 97, 493–497.

[18] McGee, S.M. (1958) Histochemical methods for calcium. J. Histochem. 6, 2241.

[19] Yamamoto, Y., Ohsaki, Y., Goto, T., Nakasima, A. and Iijima, T. (2003) Effects of static magnetic fields on bone formation in rat osteoblast cultures. J. Dent. Res. 82, 962–966.

[20] Gregoire, F.M., Smas, C.M. and Sul, H.S. (1998) Understanding adipocyte differentiation. Physiol. Rev. 78, 783–809.

[21] Katayama, K., Wada, K., Miyoshi, H., Ohashi, K., Tachibana, M., Furuki, R., Mizuguchi, H., Hayakawa, T., Nakajima, A., Kadowaki, T., Tsutsumi, Y., Nakagawa, S., Kamisaki, Y. and Mayumi, T. (2004) RNA interfering approach for clarifying the PPARγ pathway using lentiviral vector expressing short hairpin RNA. FEBS Lett. 560, 178–182.

[22] Hosono, T., Mizuguti, H., Katayama, K., Koizumi, N., Kawabata, K., Yamaguchi, T., Nakagawa, S., Watanabe, Y., Mayumi, T. and Hayakawa, T. (2005) RNA interference of PPARγ using fiber-modified adenovirus vector efficiently suppresses preadipocyte-to-adipocyte differentiation in 3T3-L1 cells. Gene 348, 157–165.

[23] Yamashita, A., Takada, T., Kanbe-Omatsu, M., Nemoto, K., Matsuura, H., Yamamoto, G. and Torii, R. (2006) Monkey embryonic stem cells differentiate into adipocytes in vitro. Cloning Stem Cells 8, 3–9.

[24] Zur Nieden, N.I., Kempka, G. and Ahr, H.J. (2003) In vitro differentiation of embryonic stem cells into mineralized osteoblasts. Differentiation 71, 18–27.